Published in final edited form as:
Dev Cell. 2013 March 11; 24(5): 554–561. doi:10.1016/j.devcel.2013.01.024.

mir-125a-5p-mediated Regulation of *Lfng* is Essential for the Avian Segmentation Clock

Maurisa F. Riley[1], **Matthew S. Bochter**[1], **Kanu Wahi**[1], **Gerard J. Nuovo**[2], and **Susan E. Cole**[1]
[1]Department of Molecular Genetics, The Ohio State University, Columbus, OH 43210
[2]Department of Pathology, Ohio State University Medical Center, Columbus, OH 43210

Summary

Somites are embryonic precursors of the axial skeleton and skeletal muscles, and establish the segmental vertebrate body plan. Somitogenesis is controlled in part by a segmentation clock that requires oscillatory expression of genes including Lunatic fringe (*Lfng*). Oscillatory genes must be tightly regulated both at the transcriptional and post-transcriptional levels for proper clock function. Here we demonstrate that microRNA-mediated regulation of *Lfng* is essential for proper segmentation during chick somitogenesis. We find that *mir-125a-5p* targets evolutionarily conserved sequences in the *Lfng* 3′UTR, and that preventing interactions between *mir-125a-5p* and *Lfng* transcripts *in vivo* causes abnormal segmentation and perturbs clock activity. This provides strong evidence that miRNAs function in the post-transcriptional regulation of oscillatory genes in the segmentation clock. Further, this demonstrates that the relatively subtle effects of miRNAs on target genes can have broad effects in developmental situations that have critical requirements for tight post-transcriptional regulation.

Introduction

Somites are cohorts of cells that bud from the anterior end of the presomitic mesoderm (PSM) and give rise to the axial skeleton and other structures (reviewed in Hirsinger et al., 2000). During somitogenesis, the expression levels of numerous genes oscillate in the PSM as part of a segmentation clock that controls the timing of somite formation. The Notch target *c-hairy1* was the first gene found expressed in this pattern (Palmeirim et al., 1997). In mouse and chick, a key oscillatory gene is Lunatic fringe (*Lfng*), which encodes a glycosyltransferase that modulates Notch signaling (Moloney et al., 2000). During vertebrate segmentation, both *Lfng* transcript levels and LFNG protein levels oscillate with a period that matches the rate of somite formation (2 hours in the mouse, 90 minutes in the chick) (Dale et al., 2003; Pourquie, 2001).

Either loss of *Lfng* expression, or sustained, non-oscillatory *Lfng* activity perturbs somite formation and patterning, presumably by altering its oscillatory expression (Dale et al., 2003; Evrard et al., 1998; Serth et al., 2003; Zhang and Gridley, 1998). It is known that cyclic *Lfng* expression is regulated at the transcriptional level (Cole et al., 2002), but little is known about the post-transcriptional mechanisms that contribute to the rapid oscillations.

Correspondence addressed to S.E. Cole (cole.354@osu.edu; Phone: 614-292-3276)..

Stable oscillatory expression patterns have been proposed to be regulated by feedback inhibition mechanisms coupled with transcriptional time delays (Lewis, 2003; Monk, 2003). Some mathematical models of the segmentation clock invoke delayed feedback loops involving regulation of Notch1, *Lfng* and *Hes7* (or *c-hairy1* in chick). In these models, mRNA and protein half-lives of oscillatory genes must be tightly regulated to ensure proper clock function (Feng and Navaratna, 2007; Gonzalez and Kageyama, 2009). The *Lfng* 3′UTR is evolutionarily conserved, and has been proposed to regulate RNA half-life (Chen et al., 2005; Hilgers et al., 2005). One possible source of such regulation would be miRNAs, non-coding RNA molecules that direct post-transcriptional repression of protein-coding genes by promoting RNA turnover and/or by decreasing translational efficiency of their target transcripts (reviewed in Bartel, 2004), and one model of oscillatory gene expression has proposed miRNA functions in the clock (Xie et al., 2007).

We hypothesized that the oscillatory expression of *Lfng* in the segmentation clock could require post-transcriptional regulation by miRNAs. Here we identify an miRNA (*mir-125a-5p*) that is enriched in the PSM, and targets evolutionarily conserved sequences in the *Lfng* 3′UTR. Inhibiting *mir-125a-5p* function or preventing interactions between *mir-125a-5p* and endogenous *Lfng* transcripts *in vivo* perturbs somitogenesis and disrupts clock function in the PSM of developing chick embryos. These findings support the hypothesis that regulation of oscillatory genes by miRNAs may provide a mechanism for post-transcriptional control of the segmentation clock.

Results

mir-125a-5p is expressed in the PSM and targets the *Lfng* 3′UTR

To examine the possibility that *Lfng* oscillations might be regulated by miRNAs, we assessed the expression of candidate miRNAs in the PSM, where the clock is active. By QRT-PCR (Fig 1A) and miRNA microarray (data not shown) we found that mir-125a-5p levels are higher in the mouse PSM, than in the mature somites. Thus, its expression is enriched in the PSM where *Lfng* is predicted to require a short RNA half life. *mir-125a-5p* is proposed to target three sites in the mouse *Lfng* 3′UTR, and one of the sites is conserved in chicken (Fig. 1B). Whole mount *in-situ* hybridization confirmed specific expression of *mir-125a-5p* in the PSM of mouse and chicken embryos (Fig 1C, panels a - c). Futher, *mir-125a-5p* expression was observed in mouse embryos in the ectoderm and mesoderm, but was largely excluded from the neural tube, notochord, and tailgut (Fig 1C, panels d and e).

The *Lfng* 3′UTR can be directly targeted by *mir-125a-5p*

To test whether *Lfng* is a direct target of *mir-125a-5p*, we examined the effects of the miRNA on transcripts containing the 3′UTR of *Lfng*. Vectors containing either mouse or chick *Lfng* 3′UTR sequence exhibit lower luciferase expression than control vectors in these cells due to the effects of endogenous miRNAs (Fig. S1A). However, expression of exogenous *mir-125a-5p* causes a further significant reduction in luciferase expression only from vectors containing the mouse or chicken *Lfng* 3′UTR (Fig. 1D-E). In contrast, mir-125a-5p binding sites were not identified in the 3′UTRs of other oscillatory genes, and *mir-125a-5p* expression had no effect on expression of transcripts containing the *Hes7* 3′UTR (Fig. S1B). Mutation of predicted *mir-125a-5p* binding sites at either end of the mouse 3′UTR, or of the single site in the chicken 3′UTR abrogates the effect of exogenous *mir-125a-5p*, indicating that *mir-125a-5p* directly interacts with the *Lfng* 3′UTR, and that these interactions are conserved among organisms that utilize *Lfng* in the segmentation clock.

Inhibition of *mir-125a-5p* activity perturbs segmentation

To dissect the function of *mir-125a-5p* in segmentation, we performed loss-of-function experiments in chick embryos using *in ovo* electroporation of antisense morpholinos to inhibit *mir-125a-5p* activity. Morpholinos complementary to *mir-125a-5p* (anti-*mir-125a*^{MO}, Supplemental Experimental Methods) bind to endogenous *mir-125a-5p*, and inhibit interactions with its target transcripts, as shown by our inability to detect *mir-125a-5p* by in situ hybridization in electroporated chick embryos (Fig S2A). 24 hours post-electroporation, the targeted region has undergone segmentation. Inhibition of *mir-125a-5p* activity perturbs formation and patterning of mature somites (n=18/18; Fig. 2). Intersomitic boundaries were absent or disorganized in the electroporated regions of the embryo (Fig. 2A). Somite patterning was also disorganized ,with reduced and diffuse expression of *Uncx4.1*, a marker of the caudal somite compartment (Fig. 2B). Inhibition of *mir-125a-5p* also leads to formation of disorganized and irregular myotome compartments, as evidenced by weak and diffuse *MyoD* expression in the electroporated region (Fig. 2C). Interestingly, phenotypes were observed even in cases where electroporations levels were comparably low. This is unlikely to be due to non-cell autonomous effects of the morpholino. Instead, it reflects one of the roles of the segmentation clock which is to synchronize the oscillations of neighboring cells. Mosaic regions of the embryo containing wild type cells mixed with cells that have altered clock function are predicted to exhibit phenotypes at the tissue level due to lack of cell:cell synchronization. This effect has recently been confirmed in mouse embryos that are chimeric for wild type and *Lfng* null cells (Okubo et al., 2012). Together, these findings indicate that *mir-125a-5p* activity is required for normal formation and patterning of epithelial somites.

mir-125a-5p activity is required for normal cyclic *Lfng* expression

We next examined the effect of *mir-125a-5p* inhibition on the expression of endogenous *Lfng. Lfng* expression was examined 2 hours post-electroporation with anti-*mir-125*^{MO}, when the targeted region of the embryo is confined to the PSM. In embryos electroporated with control morpholinos, *Lfng* expression is cyclic (Fig. 2D panels a-c). In contrast, all embryos electroporated with anti-*mir-125a*^{MO} exhibit stable *Lfng* expression in the caudal PSM as well as a band in the rostral PSM (n=15/15; Fig. 2D, panel d). The expression of a stable *Lfng* stripe in the anterior PSM may reflect the distinct control mechanisms found in the anterior and posterior PSM (Cole et al., 2002). The sustained, non-oscillatory expression of *Lfng* in the posterior PSM, where the clock is active, suggests that loss of *mir-125a-5p* activity stabilizes the *Lfng* transcript, preventing its rapid turnover.

To assess whether the change in the *Lfng* expression reflects a direct effect on endogenous *Lfng* RNA transcripts, as opposed to an indirect effect on *Lfng* transcription, we examined the expression of newly transcribed *Lfng* using an *in situ* probe for the first intron of the gene (Morales et al., 2002). In control embryos, dynamic expression of intron-containing *Lfng* transcripts is observed, with embryos exhibiting a single anterior band or an anterior band and a posterior band of varying width (Fig. 2E, panels a-b). This dynamic pattern is maintained in embryos electroporated with anti-*mir-125a*^{MO} (Fig. 2E, panels c-d), suggesting that in the short time frame of these experiments, loss of *mir-125a-5p* activity directly affects turnover of mature *Lfng* transcripts. Further, we find that the *c-hairy1* expression pattern appears oscillatory two hours post-transfection with anti-*mir-125a*^{MO} (Fig. 2F). This is expected, as *c-hairy1* oscillations have been shown to persist for one or two cycles even in the presence of cycloheximide (Palmeirim et al., 1997), thus we do not predict an overt effect on *c-hairy1* oscillations within the short time frame of this experiment, unless there are direct effects of *chairy* transcript stability. Together, these data suggest that the short term effects of *mir-125a-5p* act through effects on *Lfng* transcript stability.

Direct interactions between endogenous *mir-125a-5p* and the *Lfng* 3′UTR are required for normal somitogenesis and clock function

The segmentation phenotypes observed when *mir-125a-5p* activity is inhibited are reminiscent of those observed when *Lfng* is ubiquitously expressed in the chick PSM (Dale et al., 2003), supporting the hypothesis that *mir-125a-5p* inhibition affects *Lfng* expression. To further investigate the specificity of this effect, we directly examined the functional relevance of the *mir-125a-5p*:*Lfng* interaction, using Target Protectors (TP) (Choi et al., 2007) to specifically disrupt the binding of endogenous *mir-125a-5p* to endogenous *Lfng* transcripts in chick embryos. Target Protectors bind to miRNA recognition sites in mRNAs, physically preventing interactions between endogenous transcripts and the miRNA (Fig. 3A). A TP that binds to and blocks the *mir-125a-5p* binding site in the chick *Lfng* 3′UTR (*Lfng*-TP^{mir125a}), or a control TP complementary to a nearby conserved site in the chick 3′UTR (*Lfng*-TP^{Ctrl}) were used (Fig 3A, Supplementary Experimental Methods). In cell culture, these TPs do not themselves affect expression from transcripts containing the *Lfng* 3′UTR, but *Lfng*-TP$^{mir\text{-}125a}$ protects transcripts from the effects of exogenous *mir-125a-5p* (Fig S3), indicating that *Lfng*-TP$^{mir\text{-}125a}$ blocks binding of *mir-125a-5p* to the 3′UTR. Specifically blocking interactions between endogenous *mir-125a-5p* and *Lfng* in the chick PSM with *Lfng*-TP$^{mir\text{-}125a}$ severely perturbed segmentation. Somites were disorganized (n=21/21, Fig. 3B), with diffuse and reduced *Uncx4.1* expression (Fig. 3C). Myotome formation occurred, but compartments exhibited abnormal size and spacing reflecting underlying defects in somite morphogenesis (Fig. 3D). To examine the effects of *mir-125a-5p* on cyclic *Lfng* expression, we examined the expression of endogenous *Lfng* mRNA 2h after electroporation of target protectors. All embryos positive for *Lfng*-TP$^{mir\text{-}125a}$ exhibit strong, non-oscillatory *Lfng* expression in the caudal PSM (n= 14/14, Fig. 3E). Thus, *Lfng*TP$^{mir\text{-}125a}$ recapitulates the phenotypes seen after *mir-125a-5p* inhibition, indicating that interactions between *mir-125a-5p* and *Lfng* are essential for proper somite formation and clock function in the developing chick embryo.

Stabilization of *Lfng* transcripts affects clock function via a feedback loop

Models of the segmentation clock predict that altering the mRNA half-life of individual clock components will eventually perturb oscillations of other clock-linked genes, as the feedback loop affects the transcription of other clock components like *chairy-1* (Feng and Navaratna, 2007; Gonzalez and Kageyama, 2009; Hirata et al., 2004). To address this issue, we examined endogenous *Lfng* and *chairy-1* expression 8h (approximately 5 cycles) after electroporation. At this timepoint, all embryos positive for *Lfng*-TP$^{mir\text{-}125a}$ express *Lfng* as a single band in the anterior PSM, with no expression observed in the caudal PSM. This suggests that *Lfng* expression stabilizes at a level below our limit of detection after long term inhibition of the *mir-125a*:*Lfng* interaction (n=15/15, Fig. 4A). Disrupting interactions between *mir-125a-5p* and *Lfng* also perturbs *chairy1* oscillations, with all *Lfng*-TP$^{mir\text{-}125a}$ positive embryos exhibiting constitutive *chairy1* expression in the caudal PSM (n=15/15; Fig. 4B). This suggests that the segmentation defects observed after inhibiting *mir-125a-5p*:*Lfng* interactions result from disruption of segmentation clock function, and that altering *Lfng* transcript stability affects other clock components via feedback loops.

Discussion

Our results suggest that *mir-125a-5p* functions in post-transcriptional regulation of the chick segmentation clock by destabilizing *Lfng* transcripts. Although miRNA-based regulation in animal systems has been suggested to act largely via translational efficiency, it is clear that transcript turnover is frequently accelerated by miRNAs (Baek et al., 2008; Guo et al., 2010). Overall, our findings are consistent with a model wherein blocking interactions between *mir-125a-5p* and *Lfng* in chick embryos initially results in stabilization of *Lfng*

mRNA, although we cannot rule out that this interaction may also affect translational efficiency of the transcripts (Fig. 4C).

Because *Lfng* is a component of the oscillating clock machinery, functioning in a negative feedback loop along with Notch1 and *c-hairy-1*, the increase in *Lfng* transcript stability is predicted to have a long term effect on the expression of other clock components (Fig. 4C). Consistent with this, we observe a loss of robust oscillation of clock genes after long term inhibition of *mir-125a-5p*, with very low expression of *Lfng* in the caudal PSM (below our levels of detection by *in situ*), and a stable increase in the expression of *chairy-1* (Fig. 4C). Therefore, we propose a model where miRNAs function to regulate transcript turnover and/or translational delays in the chicken segmentation clock, facilitating the oscillatory dynamics generated by the delayed negative feedback loop during the rapid period of the clock. During the revision of this manuscript, it was reported that *mir-9* expression can influence the oscillatory expression of a Hes1 luciferase reporter in tissue culture, supporting the idea that miRNA:transcript interactions can be important in the regulation of cyclically expressed genes (Bonev et al., 2012). The work here extends this finding by altering endogenous miRNA:transcript interactions *in vivo* and revealing a robust and dramatic phenotype, supporting the hypothesis that regulation of oscillatory transcripts by miRNAs play a critical, functional role in the segmentation clock.

The conservation of this precise mechanism in other vertebrates remains unclear. Recent findings suggest that conditional inactivation of Dicer in the mesoderm of developing mouse embryos may not affect clock function in the short term (Zhang et al., 2011). However, inactivation of Dicer prevents miRNA maturation, and significant data suggests that mature miRNAs have long half-lives, ranging from 28-211 hours (Gantier et al., 2011). Thus, even after cre-mediated excision of Dicer, it is possible that cells in the PSM during early embryogenesis will still contain mature miRNAs, and that the relatively normal segmentation that was observed through E11.5 in this study could perhaps rely on residual mature miRNAs that are present in the caudal PSM cells.

We find that interfering with interactions between *mir-125a-5p* and *Lfng* transcripts *in vivo* in chick embryos stabilizes those transcripts in the PSM, suggesting an effect on RNA turnover. However, transgenic analysis examining the function of the *Lfng* 3′UTR in GFP reporter transgenes suggests that the *mir-125a-5p* binding sites may not have a dramatic effect on the 3′UTR's ability to destabilize an mRNA stability in the mouse PSM (data not shown). The possibility that the clock function of *mir-125a-5p* might not be conserved between mouse and chicken would not be surprising given that different organisms can utilize completely distinct sets of protein components in their segmentation clocks (Krol et al., 2011). Thus, it is possible that different miRNA:transcript pairs are important in the mouse segmentation clock, or that regulation occurs via translational efficiency rather than through effects on transcript stability. Testing of these models will require targeted mutation of the *mir-125a-5p* binding sites in the *Lfng* 3′UTR at the endogenous locus, to examine whether these binding sites are required for normal mouse segmentation. However, it is attractive to hypothesize that different mechanisms of post-transcriptional clock regulation could contribute to the differences in clock period observed among distinct vertebrate species.

Experimental Procedures (Supplemental Methods online)

miRNA QRT-PCR

Total RNA was extracted from the PSM and mature somites of E 9.5 embryos and QRT-PCR was performed using Taqman primers specific for mmu-*mir-125a-5p*, 2198, PN4395309 in triplicate on at least three biologically independent replicates. Results show

mean +/− SD after normalizing expression levels of the somite samples to 1. Significance calculated by Student's T test.

In-situ Hybridization

RNA *in-situ* hybridization was performed essentially as described with mRNA probes(Shifley et al., 2008), or with DIG labeled miRCURY LNA probes (Exiqon) either in whole mount embryos(Sweetman, 2011) or in section in situs(Nuovo, 2011). Section in situs were performed essentially as described (Nuovo, 2011). Details of mRNA probes and in situ protocols are found in the online supplement.

Luciferase Assays

The mouse or chick *Lfng* 3′UTR was amplified and cloned into pMIR-REPORT™ (Ambion). PCR mutagenesis of the *mir-125a-5p* seed regions using primers described in the supplemental experimental methods was confirmed by sequencing. Luciferase assays were performed in NIH3T3 cells transfected with reporter, pSVRenilla, and precursor miRNA. Cells were assayed for luciferase activity 40h post-transfection (Promega). All values reflect at least three independent experiments. Statistical analysis was performed using two way ANOVA, with Bonferroni *post hoc.*

In ovo electroporation

Fluorescein-tagged Target Protectors and Anti-mir-morpholinos (Supplemental Experimental Methods) were ordered from Gene Tools, LLC. To reduce the chance of off target interference with other miRNAs, an antisense morpholino corresponding to the NC#1 control sequence (Ambion) was ordered for use as a control morpholino. As the NC#1 sequence does not have predicted targets in vertebrate genomes, this morpholino is unlikely to affect the activity other miRNAs, and was used in preference to a scrambled sequence morpholino that might have exhibited unexpected effects. *In ovo* electroporation was performed essentially as described (Dubrulle et al., 2001). Embryos of stage 7-8HH were used for *in ovo* electroporation. Target Protectors or anti-miR morpholinos were laid on the anterior primitive streak using a glass capillary. An electric pulse of 6V, 25 mseconds was charged three times. Embryos were incubated for 2, 8 or 24 hours prior to removal and analysis. Only embryos exhibiting robust fluorescein expression and normal morphology outside of the electroporated region were used for analysis. For these analyses, 981 embryos were electroporated, with between 15 and 60% of embryos being analyzed for any particular electroporation. A subset of embryos exhibited fluorescein positive somites on only one side of the embryo. Further protocol details are in the supplemental online methods.

Supplementary Material

Refer to Web version on PubMed Central for supplementary material.

Acknowledgments

We thank R. Wharton and A. Hopper for comments, A. Fischer for help with electroporation, and the OSUCCC Nucleic Acids core facility for QRT-PCR. This work was supported by NSF grant # IOS-0919649 and NIH grant # R03HD062722 to SEC and a Pelotonia Predoctoral Fellowship to MFR.

References

Baek D, J. V, Shin C, Camargo FD, Gygi SP, Bartel DP. The impact of microRNAs on protein output. Nature. 2008; 455:64–71. [PubMed: 18668037]

Bartel D. MicroRNAs: genomics, biogenesis, mechanism, and function. Cell. 2004; 116:281–297. [PubMed: 14744438]

Bonev B, Stanley P, Papalopulu N. MicroRNA-9 Modulates Hes1 Ultradian Oscillations by Forming a Double-Negative Feedback Loop. Cell Rep. 2012; 2:10–18. [PubMed: 22840391]

Bray N, Dubchak I, Pachter L. AVID: A global alignment program. Genome Res. 2003; 13:97–102. [PubMed: 12529311]

Chen J, Kang L, Zhang N. Negative feedback loop formed by Lunatic fringe and Hes7 controls their oscillatory expression during somitogenesis. Genesis. 2005; 43:196–204. [PubMed: 16342160]

Choi WY, Giraldez AJ, Schier AF. Target protectors reveal dampening and balancing of Nodal agonist and antagonist by miR-430. Science. 2007; 318:271–274. [PubMed: 17761850]

Cole SE, Levorse JM, Tilghman SM, Vogt TF. Clock regulatory elements control cyclic expression of Lunatic fringe during somitogenesis. Dev Cell. 2002; 3:75–84. [PubMed: 12110169]

Dale JK, M. M, Dequeant ML, Malapert P, McGrew M, O. P. Periodic notch inhibition by lunatic fringe underlies the chick segmentation clock. Nature. 2003; 421:275–278. [PubMed: 12529645]

Dubrulle J, McGrew MJ, Pourquié O. FGF signaling controls somite boundary position and regulates segmentation clock control of spatiotemporal Hox gene activation. Cell. 2001; 106:219–232. [PubMed: 11511349]

Evrard YA, Lun Y, Aulehla A, Gan L, Johnson RL. Lunatic fringe is an essential mediator of somite segmentation and patterning. Nature. 1998; 394:377–381. [PubMed: 9690473]

Feng P, Navaratna M. Modelling periodic oscillations during somitogenesis. Math Biosci Eng. 2007; 4:661–673. [PubMed: 17924717]

Gantier MP, McCoy CE, Rusinova I, Saulep D, Wang D, Xu D, Irving AT, Behlke MA, Hertzog PJ, Mackay F, Williams BR. Analysis of microRNA turnover in mammalian cells following Dicer1 ablation. Nucleic Acids Res. 2011

Gonzalez A, Kageyama R. Hopf bifurcation in the presomitic mesoderm during the mouse segmentation. J Theor Biol. 2009; 259:176–189. [PubMed: 19236883]

Guo H, Ingolia NT, Weissman JS, Bartel DP. Mammalian microRNAs predominantly act to decrease target mRNA levels. Nature. 2010; 466:835–840. [PubMed: 20703300]

Hilgers V, Pourquié O, Dubrulle J. In vivo analysis of mRNA stability using the Tet-Off system in the chicken embryo. Dev Biol. 2005; 284:292–300. [PubMed: 15993405]

Hirata H, Bessho Y, Kokubu H, Masamizu Y, S. Y, Lewis J, Kageyama R. Instability of Hes7 protein is crucial for the somite segmentation clock. Nat Genet. 2004; 36:750–754. [PubMed: 15170214]

Hirsinger E, Jouve C, Dubrulle J, O. P. Somite formation and patterning. Int Rev Cytol. 2000; 198:1–65. [PubMed: 10804460]

Krol AJ, Roellig D, Dequeant ML, Tassy O, Glynn E, Hattem G, Mushegian A, Oates AC, Pourquie O. Evolutionary plasticity of segmentation clock networks. Development. 2011; 138:2783–2792. [PubMed: 21652651]

Lewis J. Autoinhibition with transcriptional delay: a simple mechanism for the zebrafish somitogenesis oscillator. Curr Biol. 2003; 13:1398–1408. [PubMed: 12932323]

Moloney DJ, Panin VM, Johnston SH, Chen J, Shao L, Wilson R, Wang Y, Stanley P, Irvine KD, Haltiwanger RS, Vogt TF. Fringe is a glycosyltransferase that modifies Notch. Nature. 2000; 406:369–375. [PubMed: 10935626]

Monk N. Oscillatory expression of Hes1, p53, and NF-kappaB driven by transcriptional time delays. Curr Biol. 2003; 13:1409–1413. [PubMed: 12932324]

Morales AV, Yasuda Y, Ish-Horowicz D. Periodic Lunatic fringe expression is controlled during segmentation by a cyclic transcriptional enhancer responsive to notch signaling. Dev Cell. 2002; 3:63–74. [PubMed: 12110168]

Nuovo GJ. In situ detection of microRNAs in paraffin embedded, formalin fixed tissues and the co-localization of their putative targets. Methods. 2011; 52:307–315. [PubMed: 20723602]

Okubo Y, Sugawara T, Abe-Koduka N, Kanno J, Kimura A, Saga Y. Lfng regulates the synchronized oscillation of the mouse segmentation clock via trans-repression of notch signalling. Nat Commun. 2012; 3:1141. [PubMed: 23072809]

Palmeirim I, Henrique D, Ish-Horowicz D, Pourquie O. Avian hairy gene expression identifies a molecular clock linked to vertebrate segmentation and somitogenesis. Cell. 1997; 91:639–648. [PubMed: 9393857]

Pourquie O. The vertebrate segmentation clock. J Anat. 2001; 199:169–175. [PubMed: 11523819]

Pourquie O, Tam PP. A nomenclature for prospective somites and phases of cyclic gene expression in the presomitic mesoderm. Dev Cell. 2001; 1:619–620. [PubMed: 11709182]

Serth K, Schuster-Gossler K, Cordes R, Gossler A. Transcriptional oscillation of lunatic fringe is essential for somitogenesis. Genes Dev. 2003; 17:912–925. [PubMed: 12670869]

Shifley ET, Vanhorn KM, Perez-Balaguer A, Franklin JD, Weinstein M, Cole SE. Oscillatory lunatic fringe activity is crucial for segmentation of the anterior but not posterior skeleton. Development. 2008; 135:899–908. [PubMed: 18234727]

Sweetman D. In Situ Detection of microRNAs in Animals. Methods Mol Biol. 2011; 732:1–8. [PubMed: 21431701]

Xie ZR, Yang HT, Liu WC, Hwang MJ. The role of microRNA in the delayed negative feedback regulation of gene expression. Biochem Biophys Res Commun. 2007; 358:722–726. [PubMed: 17509530]

Zhang N, Gridley T. Defects in somite formation in Lunatic fringe deficient mice. Nature. 1998; 394:374–377. [PubMed: 9690472]

Zhang Z, O'Rourke JR, McManus MT, Lewandoski M, Harfe BD, Sun X. The microRNA-processing enzyme Dicer is dispensable for somite segmentation but essential for limb bud positioning. Dev Biol. 2011; 351:254–265. [PubMed: 21256124]

Highlights

- *mir-125a-5p* affects the stability of *Lfng* transcripts in the chick PSM
- Inhibiting *mir-125a-5p*:*Lfng* binding perturbs the segmentation clock in chickens
- Oscillatory *Lfng* expression in the clock requires *mir-125a-5p* activity
- Loss of *mir-125a-5p* activity causes abnomal segmentation in chick embryos

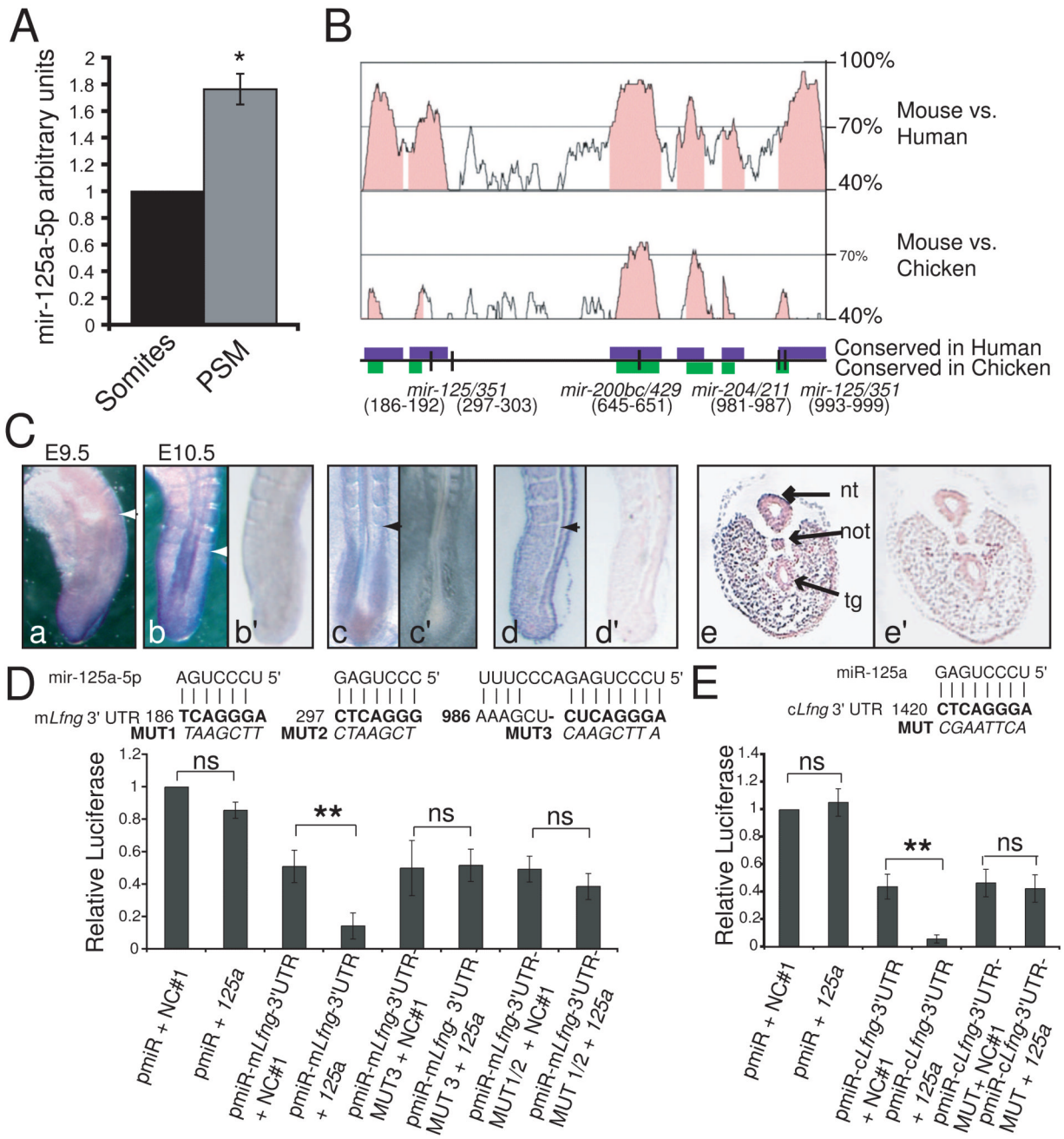

Figure 1.

The *Lfng* 3′UTR is an evolutionarily conserved target of *mir-125a-5p* **A.** By QRT-PCR *mir-125a-5p* is significantly enriched in the PSM compared to the mature somites of E9.5 mouse embryos (*= p<0.05, Student's T-Test. Error bars = SD). **B.** *Lfng* 3′UTR schematic showing high conservation among mouse, human, and chicken *Lfng* 3′UTRs (mVista Bray et al., 2003). Conserved regions shown as colored boxes. Positions of TargetScan predicted miRNA binding sites define the first nt of the 3′UTR as 1.**C.** RNA *in situ* analysis of *mir-125a-5p* in whole mount mouse embryos at E9.5 (a) and E10.5 (b), and in HH10 chick embryos (c). Section *in situ* of E10.5 mouse embryos (d= saggital, e=transverse)

demonstrate *mir-125a-5p* expression in the ectoderm and mesoderm, but not in the neural tube, notochord, and tail gut. Arrows indicate most recent somite boundary, nt = neural tube, not=notochord, tg= tailgut. *In situs* with negative control probe on adjacent sections did not exhibit staining (panels b', c', d', e'). **D.** Transfection of pre*mir-125a-5p* (125a) significantly reduces luciferase expression from pmir-m*Lfng*3′UTR (pMIR-REPORT + mouse *Lfng* 3′UTR) compared to transfection of a negative control pre-mir (NC#1). Mutations of the *mir-125a-5p* binding sites at either end of the 3′UTR (MUT1-3) abrogate this effect. **E.** Transfection of pre*mir-125a-5p* significantly reduces luciferase expression from pmir-c*Lfng*3′UTR (pMIR-REPORT + chicken *Lfng* 3′UTR). Mutations in the *mir-125a-5p* (MUT) binding site abrogate this effect. Two way ANOVA, Bonferroni *post hoc*; *=p<.05, **=p<.01, error bar = SD. See Fig. S1 for related analyses.

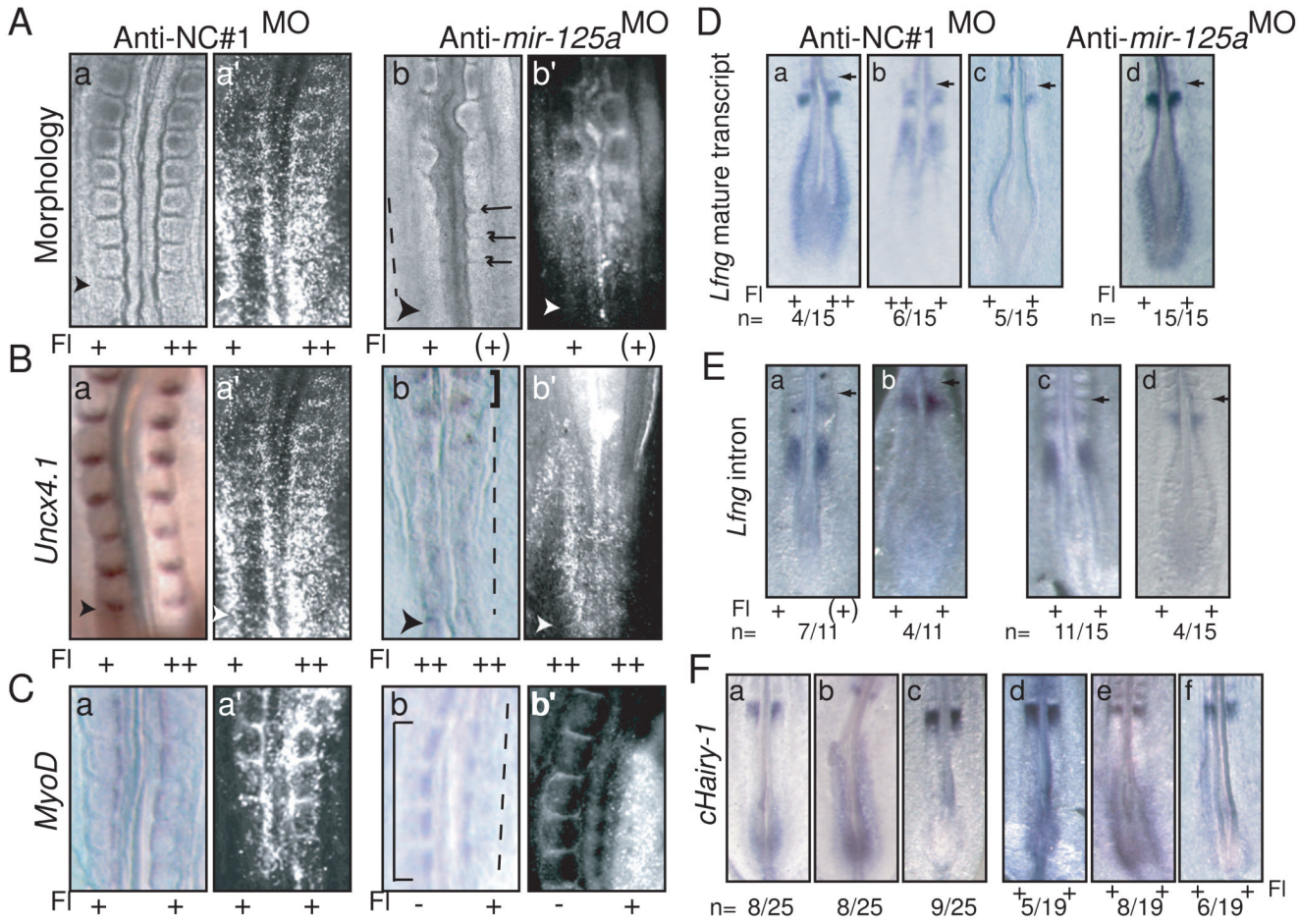

Figure 2.

Inhibition of *mir-125a-5p* perturbs somitogenesis in chicken embryos, and stabilizes *Lfng* transcripts in the PSM **A.** Electroporation of anti-NC#1MO has no effect on somite morphology (panel a), while electroporation of anti-*mir-125a*^{MO} results in abnormal somite morphology with absent (dashed line) or disorganized (arrows) intersomitic boundaries in electroporated regions (panel b).**B.** *Uncx4.1* staining is reduced and diffuse in embryos electroporated with anti-*mir-125a*^{MO} (dashed line, panel b) compared to anti-NC#1MO (panel a). Note relatively normal somites in the older region of the anti-*mir-125a*^{MO} embryo in the region that is less positive for the morpholino (square bracket). The same embryo is pictured in part A panel a and part B panel a **C.** *MyoD* expression is disorganized in somites electroporated with anti-*mir-125a*^{MO} (dashed line, panel b) compared to embryos electroporated with anti-NC#1MO (panel a). Note normal myotomes in the unelectroporated regions of the anti-*mir-125a*^{MO} embryo (square brackets). **D** 2h post-electroporation with anti-NC#1MO, endogenous *Lfng* is observed in the three described phases (Pourquie and Tam, 2001). In contrast, in anti-*mir-125a*^{MO} positive embryos, robust, non-cyclic *Lfng* expression is observed in the caudal PSM of all embryos (panel d, n=15/15). **E** *In situ* analysis with a probe specific for the *Lfng* intron demonstrates that both control embryos (a,b) and embryos electroporated with anti-*mir-125a*^{MO} (c,d) exhibit dynamic patterns of newly transcribed *Lfng* RNA. **F.** *c-hairy1* expression is cyclic in control embryos (a-c), or in embryos electroporated with anti-*mir-125a*^{MO} (d-f)Right hand panels reflect the fluorescein signal demarcating the electroporated regions of each embryo. Fl: fluorescein. Degree of

electroporation efficiency designated as “++ ” = strong, “+” = moderate, “(+)” = weak,“ −” = negative. Arrowheads indicate the most recent somite boundary. See figure S2 for fluorescein images as well as analysis of *mir-125a-5p* by *in situ* in electroporated embryos.

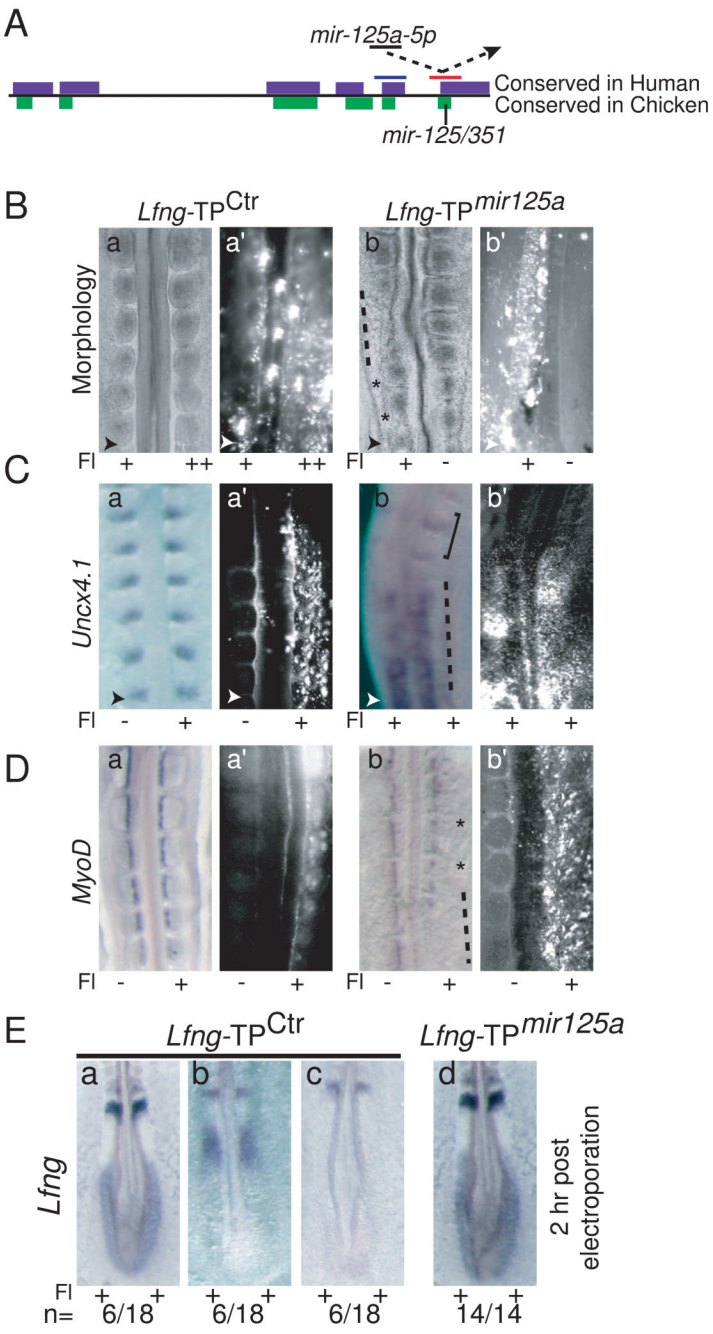

Figure 3.

Blocking interactions between *mir-125a-5p* and *Lfng* perturbs somitogenesis and segmentation clock function. **A.** Schematic of the *Lfng* 3′UTR and the TPs used, with the single *mir-125a-5p* binding site in chicken. Approximate positions of *Lfng*-TP^{Ctrl} (blue) and *Lfng*-TP$^{mir\text{-}125a}$ (red) are shown (not to scale). **B.** Electroporation of *Lfng*-TP^{ctr} has no effect on somite morphology (panels a, a'), while electroporation of *Lfng*-TP$^{mir\text{-}125a}$ results in abnormal somite morphology with absent (dashed lines) or disorganized (*) intersomitic boundaries (panels b, b'). **C.** *Uncx4.1* expression is disorganized and sometimes reduced in *Lfng*-TP$^{mir\text{-}125a}$ positive embryos (dashed line, panels b, b') compared to embryos

electroporated with *Lfng*-TP^{ctr} (panels a, a'). Note relatively normal somites in the less positive region of panel b (square bracket) **D.** *MyoD* expression in the somites of *Lfng*-TP$^{mir\text{-}125a}$ positive embryos (panels b, b') indicates that myotomes are formed, but somite compartments are of irregular sizes (*) compared to embryos electroporated with *Lfng*-TP^{ctr} (panel a, a'). In some regions of the embryo, *MyoD* expression is strongly downregulated or delayed (dashed line, panel b). **E.** 2h post-electroporation, cyclic expression of endogenous *Lfng* is observed in *Lfng*-TP^{Ctrl} embryos (panels a-c), while robust, non-cyclic *Lfng* expression is observed in the caudal PSM of *Lfng*-TP$^{mir\text{-}125a}$ positive embryos (panel d, n=14/14). Fl: fluorescein as described in Fig. 2. Arrowheads indicate the most recent somite boundary. See Fig. S3 for analysis of target protector activity in cell lines, and Fig. S4 for fluorescein images.

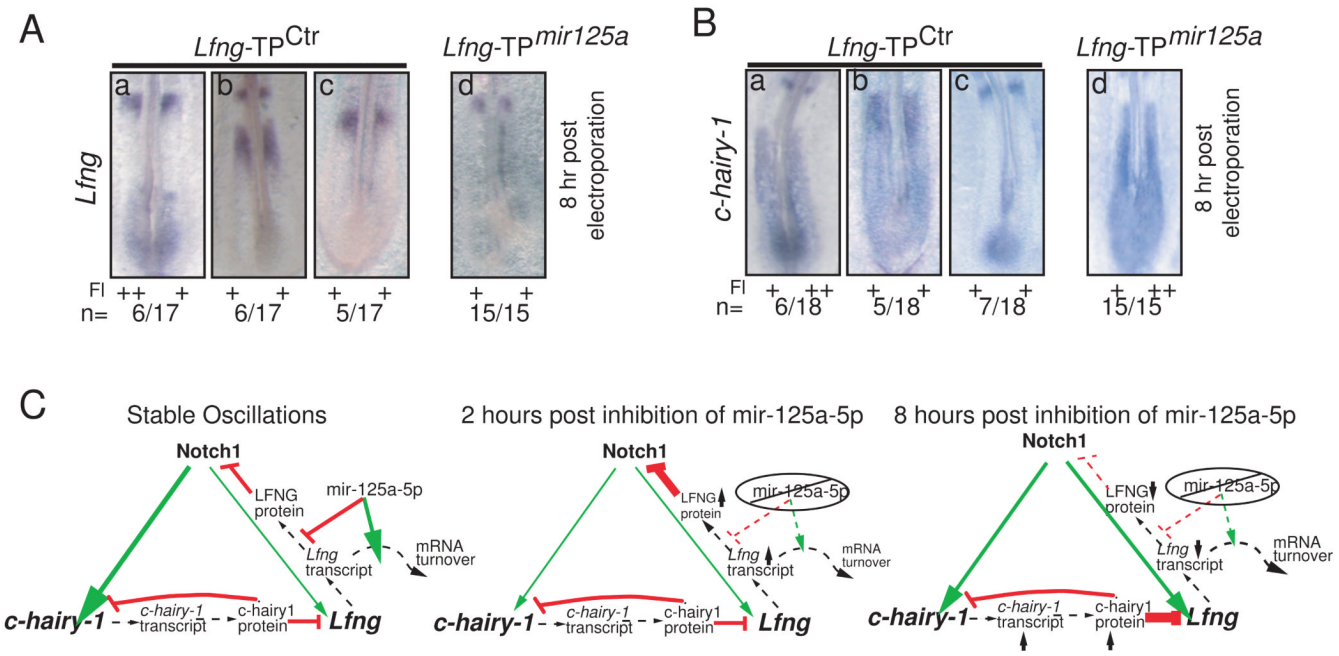

Figure 4.

Long term inhibition of interactions between *mir-125a-5p* and *Lfng* perturbs the oscillatory expression of genes linked to the segmentation clock via feedback. **A.** 8h post-electroporation, cyclic expression of endogenous *Lfng* is observed in *Lfng*-TP^{Ctrl} embryos (a-c) while endogenous *Lfng* expression is non-cyclic, with no expression detected in the caudal PSM of *Lfng*-TP$^{mir\text{-}125a}$ positive embryos (panel d, n=15/15). **B.** 8h post-electroporation, cyclic expression of endogenous *chairy1* is observed in *Lfng*-TP^{Ctrl} embryos (panels a-c), but non-cyclic *cHairy* expression is observed in the caudal PSM of *Lfng*-TP$^{mir\text{-}125a}$ positive embryos (panel d, n=15/15). Fl: Fluorescein; '+' and '++' indicate relative levels of fluorescein signal, images available in Fig S4. **C** Model for effects of *mir-125a-5p* in the clock. Stable clock oscillations are governed in part by interlocking feedback loops where Notch activates *Lfng* and *c-hairy-1* (green arrows), while LFNG protein inhibits Notch signalling, and c-hairy-1 protein inhibits its own transcription and that of *Lfng* (red lines). The lengths of delays imposed by transcription rate and translational efficiency (dashed lines), as well as the half-lives of transcripts and proteins are critical for maintenance of stable oscillations. *mir-125a-5p* is proposed to increase the rate of *Lfng* transcript turnover and/or decrease the efficiency of translation. In the absence of *mir-125a-5p*, (middle) levels of *Lfng* transcript and LFNG protein increase. In the long term (right), the effect of increased *Lfng* transcript stability is loss of robust oscillations, with stable, increased levels of *c-hairy-1* transcript, and stable decreased transcription of *Lfng*. See also Fig. S4 for fluorescein images